Progress of Theoretical Physics, Vol. 60, No. 1, July 1978

# The Effects of the $1p_{3/2}$ Core Excitations on the Properties of the $N=50$ Isotones

Kazuhisa FUJITA and Toshiya KOMODA

*Department of Physics, College of Science and Engineering, Aoyama Gakuin University, Tokyo 157*

(Received November 16, 1977)

The low-lying energy levels and various transition rates of six $N=50$ isotones from $^{89}$Y to $^{94}$Ru are calculated in the configuration space including one and two proton excitations from the $1p_{3/2}$ core orbit in addition to the $(0g_{9/2}, 1p_{1/2})^n$ configuration. Some particular levels, e.g., the second $2^+$ state in $^{90}$Zr, the first $7/2^+$ and the second $3/2^-$ states in $^{91}$Nb and almost all low-lying states in $^{89}$Y, etc., are well explained by the present model. The effect of this extension of the configuration space is reflected more strongly on the transition rates. Especially, by taking account of the core excitation from the $1p_{3/2}$ orbit, the rates of the $M1$ and $E3$ transitions which are forbidden in the $(0g_{9/2}, 1p_{1/2})^n$ configuration space can be estimated. The $E0$, $E2$, $E4$, $M4$ and $E5$ transition rates in these nuclei are also calculated and compared with the experimental data. In some particular transitions in the heavier nuclei, the drastic discrepancies are obtained between the calculated results with and without the $1p_{3/2}$ core excitations.

## § 1. Introduction

To describe some nuclear properties of the $N=50$, $A\geqq 90$ isotones in the shell-model, it has been assumed that the $^{88}$Sr nucleus is an inert core and all low-lying states arise from the motion of several valence protons above $Z=38$ closed-shell. Such a description was first used to explain the observed level structure of $^{90}$Zr.[1),2)] Actually, the $\chi^2$-fitting method in the $(0g_{9/2}, 1p_{1/2})^n$ configuration space has been successful in the calculations of the energy levels and some other properties of the $N=50$ nuclei.[3)~8)]

Recently, however, it was pointed out that the above configuration space is not sufficient to explain some energy levels of these nuclei.[8),9)] For example, the second $2^+$ excited state in $^{90}$Zr cannot be reproduced by the $(0g_{9/2}, 1p_{1/2})^2$ configuration. It was suggested that some core excited configurations are necessary to explain the second $2^+$ state.[8)] Dedes and Irvine[10),11)] calculated the positive parity levels of this nucleus using a $2p$-$2h$ basis. In their calculation, this nucleus was dealt as a core, and two-proton excitations from the $0f$-$1p$ shell to $0g_{9/2}$ orbit were taken into account. The second $2^+$ state was well explained by their calculation. Courtney and Fortune[12)] have shown that the $E0$ transition rate between the lowest two $0^+$ states in $^{90}$Zr cannot be explained without two-proton excitation from the $1p_{3/2}$ orbit. In order to explain the detailed properties of the $N=50$ nuclei, it seems necessary to extend the configuration space.

Vergados and Kuo[13] have calculated the energy levels of $^{89}$Y taking account of both proton and neutron excitations from the $^{88}$Sr core. From their result the low-lying levels of this nucleus can be sufficiently explained without the neutron excitations. Therefore, it is expected that the low-lying levels in the $N=50$ nuclei which have several protons outside the $^{88}$Sr core can also be described by taking only proton excitations into account. Thus in the present paper, we assume that 50 neutrons form the closed shell. The purpose of our work is to study the effects of the proton excitations from the $^{88}$Sr core on the energy levels and other properties of the $N=50$ nuclei.

In § 2, the model space and the other assumptions which are adopted in our calculations are discussed. The calculated results of the energy levels and various transition rates are compared with the experimental values in §§ 3 and 4, respectively.

## § 2. The model

As discussed earlier,[9] we need to consider proton jumps from the $^{88}$Sr core to understand some nuclear properties of the $N=50$ nuclei. The single particle energies of two core orbits ($1p_{3/2}$ and $0f_{5/2}$ orbits) are expected to close by each other and, therefore, the proton jumps from both of these orbits should be taken as the core excitations. Since, however, the inclusion of every possible proton jump from these two orbits involves shell-model calculations of inhibitive immensity, we are forced to restrict the dimension of the model space. We assume that the most important core excitations are the proton jumps from the $1p_{3/2}$ orbit, and that the proton jumps from the $0f_{5/2}$ orbit can be neglected.

To clarify the effects of the core excitations, we have carried out two calculations A) and B). In the calculation A), all particles are confined to the $0g_{9/2}-1p_{1/2}$ subshell and the $1p_{3/2}$ orbit is assumed to be closed. On the other hand, in the calculation B), the core excitations are allowed, and one and two protons are permitted to jump from the $1p_{3/2}$ orbit to the $0g_{9/2}-1p_{1/2}$ subshell. The two configuration spaces employed in the calculations A) and B) are denoted symbolically as follows,

A) $(0g_{9/2}, 1p_{1/2})^{n}$ ,

B) $(0g_{9/2}, 1p_{1/2})^{n+m}(1p_{3/2})^{-m}$ ,

where $n=Z-38$ and $m=0$, 1 and 2.

In the shell-model studies within the $0g_{9/2}-1p_{1/2}$ configuration space, the effective two-body matrix elements were often deduced from the $\chi^2$-fitting method.[3)~8)] However, we are obliged to use a semiempirical interaction in this work because of lack of enough number of the experimental energy levels to carry out the $\chi^2$-fitting method in the extended configuration space. We take the Kallio-Kolltveit (K-K) interaction[14] which has a hard core and is expressed as

$$V_{12}=\frac{1}{4}(3V_t+V_s)+\frac{1}{4}(V_t-V_s)\sigma_1\cdot\sigma_2\,,$$

where the radial dependence of $V_k$ ($k=t$ or $s$) are given by

$$V_k=\begin{cases}-A_k\exp[-\alpha_k(r-c)] & r>c\,,\\ \infty & r\leqq c\,.\end{cases}$$

Suffices $t$ and $s$ indicate spin triplet and singlet, respectively. Values of the parameters are

| | $c$ (fm) | $A_k$ (MeV) | $\alpha_k$ (fm$^{-1}$) |
|---|---|---|---|
| triplet | 0.4 | 475.0 | 2.5214 |
| singlet | 0.4 | 330.8 | 2.4021 . |

These parameters are adjusted to reproduce the two-body scattering data. This interaction was successfully applied to calculate the energy levels of $^{16}O$, $^{18}O$ and $^{20}Ne$.[14),15)]

We employ the separation method[16)] with separation distances 0.925 fm for the triplet state and 1.025 fm for the singlet state to treat the hard core, and calculate two-body matrix elements using the harmonic oscillator wave function with an oscillator constant $\nu=m\omega/\hbar=0.228\,\mathrm{fm}^{-2}$. This K-K interaction was given firstly with the assumption that it acts only in the relative $s$ state.[14),15)] In this paper, however, we apply this interaction to all states with possible relative orbital angular momenta in the calculations of matrix elements in order to avoid the localization of the contribution of $s$ state interaction on the two-body matrix element with total spin $J=0$. Strictly speaking, different separation distances should be taken for different $l$ states. But the value of the Talmi integral of high $l$ state is insensitive to separation distance.

Since the purpose of this paper is to indicate *explicitly* the effect of particle jumps from the core on some properties of the $N=50$ nuclei, we do not include any correction terms due to the core polarization effect on the two-body matrix elements used in our calculations.

Single-particle energy differences $\varepsilon(0g_{9/2})-\varepsilon(1p_{1/2})$ and $\varepsilon(1p_{1/2})-\varepsilon(1p_{3/2})$ are varied in the calculation B), so as to give the best fit between the calculated and the observed energy levels of $^{89}Y$, $^{90}Zr$ and $^{91}Nb$, simultaneously. Adopted values are 1.25 MeV for $\varepsilon(0g_{9/2})-\varepsilon(1p_{1/2})$ and 0.60 MeV for $\varepsilon(1p_{1/2})-\varepsilon(1p_{3/2})$. The same value of the single-particle energy difference $\varepsilon(0g_{9/2})-\varepsilon(1p_{1/2})$ is used also in the calculation A). Therefore, any differences between the calculated results with the configurations A) and B) are directly interpreted as due to the effect of the $1p_{3/2}$ core excitations.

## § 3. Energy levels

The energy levels of six $N=50$ nuclei from $^{89}Y$ to $^{94}Ru$ are calculated in the

Table I. Binding energies relative to the $^{88}$Sr core (in MeV).[a)]

| Nucleus | A | B | Exp.[b)] |
|---|---|---|---|
| $^{89}$Y | 6.600 | 6.862 | 7.068 |
| $^{90}$Zr | 14.205 | 14.544 | 15.434 |
| $^{91}$Nb | 20.153 | 20.421 | 20.592 |
| $^{92}$Mo | 28.198 | 28.591 | 28.058 |
| $^{93}$Tc | 34.549 | 34.835 | 32.162 |
| $^{94}$Ru | 42.984 | 43.342 | 38.397 |

a) In the theoretical values, the Coulomb effects are taken into account from Ref. 17).
b) A. H. Wapstra and N. B. Gove, Nuclear Data Tables **9** (1971), 265.

two configuration spaces defined in the previous section. The results are compared with the experimental ones in Figs. 1∼3 for the even $Z$ nuclei and in Figs. 4∼6 for the odd $Z$ nuclei.

The binding energies of the ground state of these nuclei relative to the $^{88}$Sr core are shown in Table I. In the theoretical values, the Coulomb effect calculated with the harmonic oscillator model[17)] is taken into account. The agreements with the experimental ones are good except for $^{93}$Tc and $^{94}$Ru. The overestimate of the binding energies in these heavier nuclei indicates that the two-body matrix elements, especially the diagonal two-body matrix elements, used in this paper are a little too attractive. Since, however, each one of the diagonal matrix elements for the $(0g_{9/2}, 1p_{1/2})^2$ configuration of the K-K interaction shifts uniformly (about $-0.5$ MeV) from the corresponding one of the $\chi^2$-fitting calculation,[8)] the two-body matrix elements of the K-K interaction are useful to explain the low-lying energy level structure relative to the ground state energy.

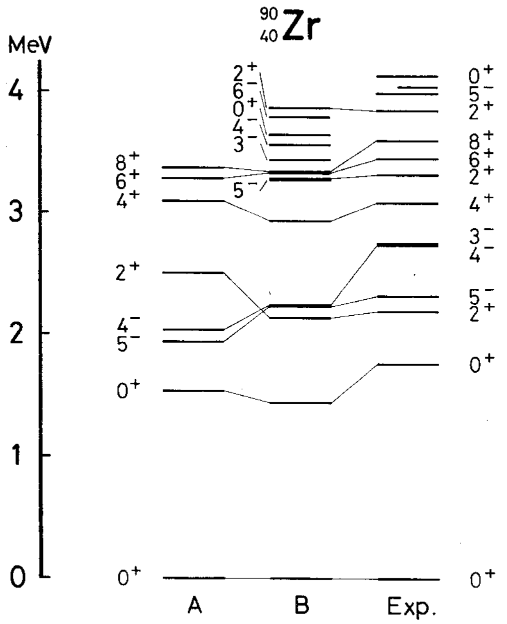


Fig. 1. Experimental and theoretical energy spectra for $^{90}$Zr. Columns A and B give our results calculated in A) configurations within the $0g_{9/2}-1p_{1/2}$ subshell and B) configurations with the $1p_{3/2}$ core excitations. All levels are shown up to 4 MeV. The experimental data are taken from Ref. 18).

## 3.1. *Even Z nuclei*

### 3.1.1. The nucleus $^{90}$Zr

As is shown in Fig. 1, the calculated energy spectrum agrees fairly well with the observed one.[18)]

In the calculation of the positive parity levels of this nucleus by Dedes,[11)] a multiplying factor named $S$ was introduced phenomenologically to improve large depression of the ground state energy. Note that in our calculation, we do not use any phenomenological assumptions such as the parameter $S$.

From comparison of the energy levels in the calculations A) and B) in Fig. 1, it is found that the $1p_{3/2}$ core excitations bring about two important effects on the low-lying energy levels of $^{90}$Zr.

Firstly, the second $2^+$ state observed at 3.33 MeV can be reproduced very well by including the $1p_{3/2}$ core excitations. The configuration with one-hole in the $1p_{3/2}$ orbit is a main component (about 71%) of this state.

Secondly, the level order between the first $2^+$ and first $5^-$ states is reproduced in the calculation B). It could not be explained within the $0g_{9/2}-1p_{1/2}$ configuration space even with the $\chi^2$-fitting method [for example, Gloeckner and Serduke, Fig. 1 of Ref. 8)]. The drastic reordering of the levels in the calculation B) is principally caused by the lowering of the first $2^+$ level. The admixture of the core excited configurations amounts to $\sim$40% in the first $2^+$ state, whereas the admixture is small (less than 20%) in the other low-lying states.

It is seen in Fig. 1 that the first $3^-$ state which appears at 2.748 MeV in experiment cannot be explained even if the $1p_{3/2}$ core excitations are taken into account. It is interpreted as the collective state induced by octupole vibration because of its small excitation energy and large $E3$ transition rate to the ground state (see Table II in § 4.1).

3.1.2. The nucleus $^{92}$Mo

The theoretical and experimental energy spectra[19),20)] of this nucleus are shown in Fig. 2.

By including the $1p_{3/2}$ core excitations, the second $0^+$ and the second $2^+$ states are strongly affected. The core excited configurations, especially the one-particle core excited configuration, have large contribution on these states. The importance of the one-particle excitation from the $1p_{3/2}$ orbit to the $1p_{1/2}$ orbit was pointed out in the calculation of the magnetic moment of the odd mass nuclei with the simple perturbation theory.[21),22)] The important effect of the one-particle core excitation is also shown in our calculation. Concerning the second $2^+$ state, the

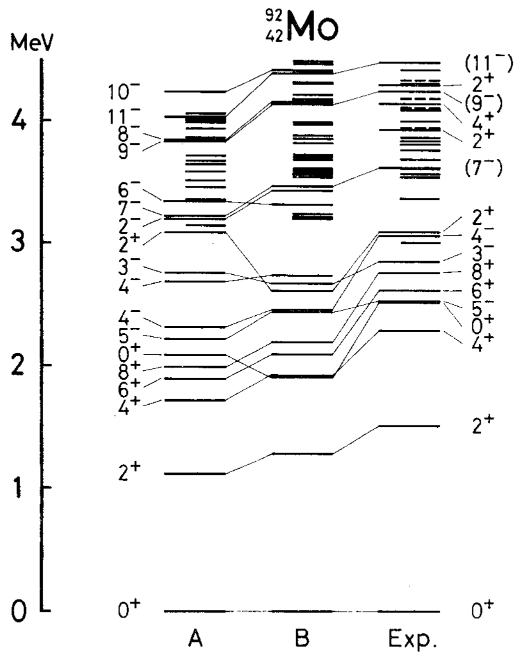


Fig. 2. Experimental and theoretical energy spectra for $^{92}$Mo. All levels are shown up to 4.5 MeV. The experimental data are taken from Refs. 19) and 20). See also the caption for Fig. 1.

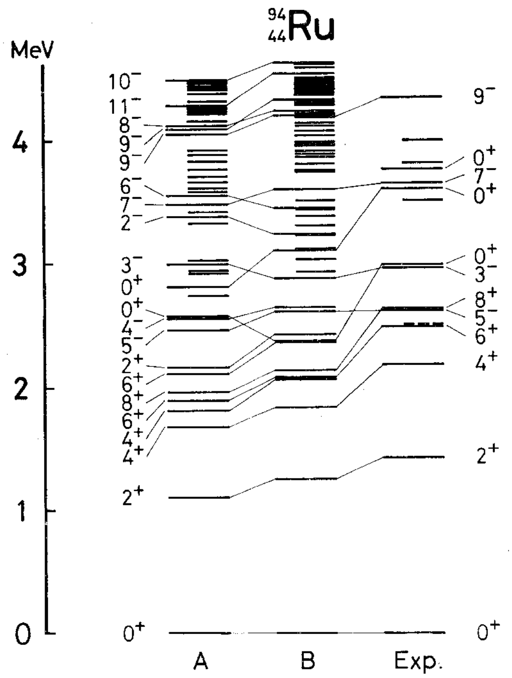


Fig. 3. Experimental and theoretical energy spectra for $^{94}$Ru. All levels are shown up to 4.5 MeV. The experimental data are taken from Refs. 20) and 24). See also the caption for Fig. 1.

$M1$ transition rate between this state and the first $2^+$ state can be interpreted to some extent by the large mixing of the one-particle core excited configuration (see § 4.1.). Moreover, the second $0^+$ state could not be reproduced by the calculation including only two-particle core excitation.[23]

The contribution of the core excitations is very small in the other low-lying positive and negative parity states except for the $3^-$ state. The mixing of the core excited configurations in the $3^-$ state is very large (about 36%), but the position of this state cannot be explained. The properties of this state should be interpreted with the other model as like as the $3^-$ state in $^{90}$Zr.

3.1.3. The nucleus $^{94}$Ru

A comparison between the theoretical and experimental energy spectra[20),21)] of this nucleus is given in Fig. 3.

It is found from Fig. 3 that the $1p_{3/2}$ core excitations affect only a little the energy levels of this nucleus. The admixtures of the core excited configurations in all low-lying states, except for the first $3^-$ and second $0^+$ states, are only a few percents. This indicates that the structure of the low-lying levels is almost explained with the $(0g_{9/2}, 1p_{1/2})^6$ configuration as in Refs. 3) ~8), and that the core excitations affect mainly the higher excited levels.

## 3.2. *Odd Z nuclei*

### 3.2.1. The nucleus $^{89}$Y

Only two single-particle states, i.e., $1/2^-$ and $9/2^+$ states, can be constructed within the $0g_{9/2}-1p_{1/2}$ configuration space. Thus the observed levels other than the above two states must be associated with the core excitations.

This nucleus has been investigated in terms of various models including the core excitations[11),25)] and the reasonable results have been obtained in these calculations. It is found that the result with our simple shell-model calculation is as good as these ones. The theoretical and experimental energy spectra[26),27)] are shown in Fig. 4.

It is seen from Fig. 4 that all low-lying levels, except the $5/2^-$ level, are well explained in the calculation B). The first $5/2^-$ state is usually taken as the $0f_{5/2}^{-1}$ state.[28),29)] The first $3/2^-$ level which is considered the $1p_{3/2}^{-1}$ state[28),29)] is well reproduced. The high-spin states, $9/2^+$ and $11/2^+$ states, etc., are also in good agreement with the experiments. Recently, the level at 2.893 MeV is assigned to $13/2^+$ state from $(p, p')$ reaction data.[27)] The corresponding state appears at 3.21 MeV in our result.

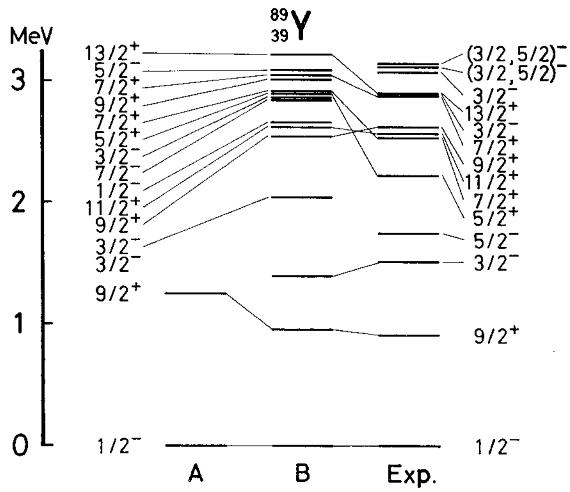


Fig. 4. Experimental and theoretical energy spectra for $^{89}$Y. All levels are shown up to 3.2 MeV. The experimental data are taken from Refs. 26) and 27). See also the caption for Fig. 1.

The second $3/2^-$ state is found at 2.884 MeV in experiments.[26)] It is expected that this state arises from the one-proton core excitation from the $1p_{3/2}$ orbit to the $0g_{9/2}$ orbit. In our result, however, the second $3/2^-$ state which has the configuration $|0g_{9/2}^2(0)\ 1p_{3/2}^{-1};\ 3/2^-\rangle$ as a main component appears at very low position (2.04 MeV). A similar result on the position of this state was also obtained in the calculation of Vergados and Kuo.[11)] This excessive low position of this $3/2^-$ state is caused mainly from the small non-diagonal matrix element between two states $|0g_{9/2}^2; 0^+\rangle$ and $|1p_{1/2}^2; 0^+\rangle$, which contributes to widen the spacing between the first and second $3/2^-$ states. Actually, this non-diagonal element used in our calculation is rather small (about one-third) than that used by Gloeckner and Serduke.[8)] The excitation energies of the first and second $3/2^-$ states relative to the ground state are well explained if we assume that non-diagonal elements between the $|0g_{9/2}^2; 0^+\rangle$ and $|j^2; 0^+\rangle$ states, where $j=1p_{1/2}$ and $1p_{3/2}$, are twice as large as the ones used in this paper. This modification may enlarge also the spacing between the ground and first excited $0^+$ states in $^{90}$Zr, but will not affect too much because of rather large spacing between these two $0^+$ states. It is expected that this modification gives also the constructive effects on some transition rates as discussed later.

### 3.2.2. The nucleus $^{91}$Nb

The theoretical and experimental energy spectra[30)~32)] are given in Fig. 5. The agreement with the experiments is much improved in the calculation B) compared with the calculation A).

The comparison of the calculations A) and B) shows that the positive parity levels are, as a whole, lowered by including the $1p_{3/2}$ core excitations. In particular, the first $7/2^+$ state is lowered considerably to explain the observed anoma-

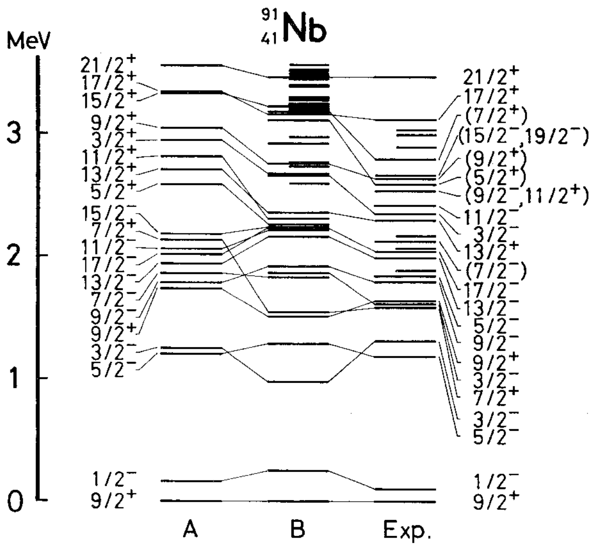


Fig. 5. Experimental and theoretical energy spectra for $^{91}$Nb. All levels are shown up to 3.6 MeV. The experimental data are taken from Refs. 30)～32). See also the caption for Fig. 1.

lously low-lying position of this state. The core excited configurations have very large contribution (about 40%) to this state. Similarly, the large admixtures of the core excited configurations occur in several high-spin positive parity states, e.g., $11/2^+$, $13/2^+$, $15/2^+$, $17/2^+$ and $21/2^+$ states. The agreement of these states with the observed ones is good. These large admixtures of the core excited configurations affect also the transition rates considerably (see § 4.2.).

On the other hand, the negative parity levels except the $3/2^-$ state are not so influenced by the $1p_{3/2}$ core excitations. The second $3/2^-$ state observed at 1.606 MeV is supposed to be $4p$-$1h$ state because of the large $1p_{3/2}$ single-particle strength in proton pick-up on $^{92}$Mo.[33] Actually, the second $3/2^-$ state is predicted at 1.870 MeV in the calculation B), whereas no such state appears in the calculation A).

Since the second $5/2^-$ state observed at 1.842 MeV is supposed to be generated from the one-proton excitation from the $0f_{5/2}$ orbit because of the large $0f_{5/2}$ single-particle strength in proton pick-up reaction,[33] this state is out of our consideration.

### 3.2.3. The nucleus $^{93}$Tc

A comparison between the theoretical and experimental energy spectra[30),34)～36)] of this nucleus is given in Fig. 6.

It seems that in this nucleus the $1p_{3/2}$ core excitations have less effect on the energy levels than in the case of $^{91}$Nb. This indicates that the low-lying energy levels are almost explained with the $(0g_{9/2}, 1p_{1/2})^5$ configuration. Only $3/2^-$ states are influenced to some extent and come down slightly. The three levels observed at 1.193, 1.499 and 1.787 MeV are tentatively assigned to be $3/2^-$ or $1/2^-$ states from ($^3$He, d) and (d, n) reaction data.[35)～38)] Our calculation shows two $3/2^-$ levels at 1.162 and 2.075 MeV, but it is not sure to which observed levels the calculated ones correspond.

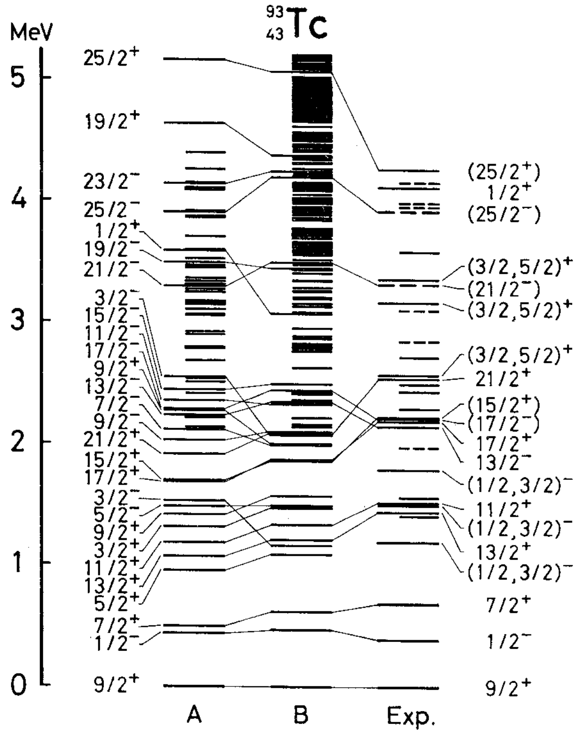


Fig. 6. Experimental and theoretical energy spectra for $^{93}$Tc. All levels are shown up to 5.2 MeV. The experimental data are taken from Refs. 30), 34)～36). See also the caption for Fig. 1.

## § 4. Transition rates

Electromagnetic transition rates of six $N=50$ nuclei are calculated with the wave functions obtained in the previous section and are compared with the experimental ones in Tables II～VIII. The radial matrix elements of the transition operator are computed in the harmonic oscillator model with the oscillator constant $\nu=0.212\,\text{fm}^{-2}$, which is used by many authors.[6),8),39),40)] All reduced transition probabilities are calculated with the free proton charge and $g$-factors without any modification. The transition rates are calculated with the wave functions of the $(0g_{9/2}, 1p_{1/2})^n$ configuration for the two-body matrix elements 'Level' proposed by Gloeckner and Serduke[8)] and are shown also in these tables, for comparison.

Some transitions are not allowed when the configuration space is restricted to $(0g_{9/2}, 1p_{1/2})^n$. For example, $M1$ transition between the positive parity states is forbidden, since the states are described with the $|0g_{9/2}^{n-2}(v, J)\,1p_{1/2}^2(0)\,;J^+\rangle$ and $|0g_{9/2}^n;\,vJ^+\rangle$ configurations and the $M1$ transition operator is effectively proportional to the total angular momentum $J$ in these states. $E3$ transition is also forbidden, because this transition cannot occur between the $1p_{1/2}$ and $0g_{9/2}$ orbits. In the calculation of the magnetic moment with the simple perturbation theory,[21),22)] the importance of the one-particle excitation from the $1p_{3/2}$ orbit to the $1p_{1/2}$ orbit was pointed out. Similarly, taking account of the core excitations from the $1p_{3/2}$ orbit, we can obtain non-vanishing matrix elements of $M1$ and $E3$ transitions.

The $E0$, $E2$, $E4$, $M4$ and $E5$ transition rates are also calculated with and without the core excitations and compared with the experimental data. Some of these transition rates are improved fairly well by taking account of the $1p_{3/2}$ core excitations as shown later.

4.1. *Transition rates in even Z nuclei*

It is seen from Table II that, in $^{90}$Zr, the $M1$, $E2$ and $E3$ transitions are affected considerably by the $1p_{3/2}$ core excitations. Concerning the calculated $B(E2)$ values, the large enhancement occurs in the $4^+\to2_1^+$ and $2_1^+\to0_2^+$ transitions, but the enhancement of the $8^+\to6^+$ and $6^+\to4^+$ transitions is rather small. In the low-spin positive parity states (i.e., $0^+$, $2^+$ and $4^+$ states), the $B(E2)$ values are increased by large admixtures of the one-proton core excited configura-

Table II. Reduced transition probabilities $B(\sigma L)$[a)] in $^{90}$Zr.

| $\sigma L$ | $J_i\to J_f$ | $B(\sigma L)_{\rm exp}$ | $B(\sigma L)_A$ | $B(\sigma L)_B$ | $B(\sigma L)_{\chi^2}$[b)] |
|---|---|---|---|---|---|
| $M1$ | $2_2^+\to2_1^+$ | | — | $5.62\times10^{-2}$ | — |
| | $4^-\to5^-$ | | $5.45\times10^{-1}$ | 1.19 | $5.45\times10^{-1}$ |
| $E2$ | $2_3^+\to0_1^+$ | 49[c)] | — | 1.70 | — |
| | $8^+\to6^+$ | $60.5\pm2.5$[d)] | 16.53 | 25.04 | 16.53 |
| | $6^+\to4^+$ | | 41.27 | 76.67 | 41.27 |
| | $2_2^+\to0_2^+$ | | — | 3.62 | — |
| | $\to0_1^+$ | | — | 0.93 | — |
| | $4^+\to2_1^+$ | | 59.68 | 122.80 | 59.68 |
| | $2_1^+\to0_2^+$ | 150[c)] | 49.02 | 96.48 | 33.38 |
| | $\to0_1^+$ | 135[c),e)] | 2.91 | 15.49 | 18.56 |
| $E4$ | $4^+\to0_1^+$ | $\approx3.8\times10^4$ [f)] | $1.42\times10^3$ | $2.74\times10^3$ | $9.06\times10^3$ |
| $E3$ | $8^+\to5^-$ | $31\pm3$[g)] | — | 42.18 | — |
| | $3^-\to0_1^+$ | $(15.4\pm0.4)\times10^3$ [h)] | — | $2.01\times10^3$ | — |
| | $5^-\to2_1^+$ | | — | 2.31 | — |
| $E5$ | $5^-\to0_2^+$ | | $5.80\times10^5$ | $7.98\times10^5$ | $1.18\times10^6$ |
| | $\to0_1^+$ | $33\times10^6$ [i)] | $9.65\times10^5$ | $1.11\times10^6$ | $3.68\times10^5$ |

a) $B(EL)$ values are given in units of $e^2\cdot{\rm fm}^{2L}$ and $B(ML)$ values in units of $\mu_0^2\cdot{\rm fm}^{2(L-1)}$.
b) These values are calculated with the wave functions for the $\chi^2$-fitting two-body matrix elements 'Level' in Ref. 8).
c) Ref. 18).
d) Ref. 46).
e) Ref. 45).
f) Ref. 47).
g) Ref. 44).
h) Ref. 42).
i) Ref. 48).

tion $|0g_{9/2}^2(J-2)1p_{1/2}1p_{3/2}^{-1}; J^+\rangle$ which has non-vanishing $E2$ matrix element with the leading component in the $(J-2)^+$ state, i.e., $|0g_{9/2}^2; J-2^+\rangle$. On the other hand, in the high-spin positive parity states (i.e., $6^+$ and $8^+$ states), the mixing of the above one-proton core excited configuration is not large.

Rather strong observed $E2$ transitions from the first and third $2^+$ states to the ground state and $E4$ transition from the first $4^+$ state to the ground state are not reproduced even in the extended model space including the $1p_{3/2}$ core excitations. These are caused by the fact that the ground state is dominated by the configuration $|1p_{1/2}^2; 0^+\rangle$ in our calculation. No configurations which have non-vanishing $E2$ and $E4$ matrix elements with this configuration appear in the $2^+$ and $4^+$ states even in the extended model space. To explain the above transition rates, the modification of the two-body matrix elements mentioned before (see § 3.2.1) may be necessary because this will decrease the amplitude of the $|1p_{1/2}^2; 0^+\rangle$ component and, instead, increase that of the $|0g_{9/2}^2; 0^+\rangle$ component in the ground state.

Table III. Matrix elements $|M|$[a)] of electric monopole transition in $^{90}$Zr.

| $\sigma L$ | $J_i \to J_f$ | $\lvert M\rvert_{exp}$ (fm$^2$) | $\lvert M\rvert_A$ (fm$^2$) | $\lvert M\rvert_B$ (fm$^2$) | $\lvert M\rvert_{\chi^2}$ (fm$^2$) |
|---|---|---|---|---|---|
| $E0$ | $0_2^+ \to 0_1^+$ | 1.60±0.04[b)] | 2.17 | 2.89 | 4.52[c)] |

a) $|M| = |\langle f|\Sigma_p r_p^2|i\rangle|$.
b) Ref. 12).
c) This value is calculated with the wave function for the $\chi^2$-fitting two-body matrix elements 'Level' in Ref. 8).

The $B(E3)$ value for the $8^+ \to 5^-$ transition is well explained by our calculation. The $B(E3)$ value is very sensitive to the mixings of the core excited configurations as already mentioned. Since the $5^-$ state is dominated by the configuration $|0g_{9/2} 1p_{1/2}; 5^-\rangle$, the mixing of the one-proton core excited configuration of about 13% in the $8^+$ state is important to explain this transition in our calculation.

To explain the $3^- \to 0_1^+$ transition quantitatively, more extension of the shell-model space is necessary because of the highly collective nature of the $3^-$ state (see § 3.1.1).

The $E0$ transition is observed between the first excited $0^+$ and ground $0^+$ states in $^{90}$Zr (Table III). Courtney and Fortune[12)] indicated using the wave functions deduced from the experimental spectroscopic factors that this $E0$ matrix element can be explained including the two-proton core excitation from the $1p_{3/2}$ orbit. In our calculation, however, it seems that the result is not sensitive to the mixing of the core excited configurations. Calculation A) (without core excitation) is a little more favorable than calculation B).

In $^{92}$Mo (Table IV), recently, the $B(M1)$ for the $2_2^+ \to 2_1^+$ transition was

Table IV. Reduced transition probabilities $B(\sigma L)$[a] in $^{92}$Mo.

| $\sigma L$ | $J_i \to J_f$ | $B(\sigma L)_{\text{exp}}$ | $B(\sigma L)_A$ | $B(\sigma L)_B$ | $B(\sigma L)_{\chi^2}$[b] |
|---|---|---|---|---|---|
| $M1$ | $2_2^+ \to 2_1^+$ | $\left(6.3^{+2.0}_{-1.8}\right)\times 10^{-2}$ [c] | 0. | $8.85\times10^{-4}$ | 0. |
| | $4^- \to 5^-$ | | $5.45\times10^{-1}$ | $6.87\times10^{-1}$ | 0. |
| $E2$ | $2_2^+ \to 2_1^+$ | $143^{+57}_{-54}$ [c] | 0.52 | 0.09 | 3.32 |
| | $\to 0_1^+$ | $75^{+22}_{-54}$ [c] | 0.87 | 5.91 | 2.21 |
| | $8^+ \to 6^+$ | $32.4\pm1.2$ [d] | 16.08 | 15.07 | 12.05 |
| | $6^+ \to 4^+$ | $78.5\pm2.5$ [d] | 40.18 | 37.19 | 29.84 |
| | $0_2^+ \to 2_1^+$ | | 0.66 | 2.69 | 0. |
| | $4^+ \to 2_1^+$ | $<583$ [c] | 58.10 | 52.84 | 42.93 |
| | $2_1^+ \to 0_1^+$ | $234\pm40$ [e] | 52.31 | 59.03 | 58.13 |
| | $11^- \to 9^-$ | $85\pm5$ [f] | 33.05 | 42.79 | 33.05 |
| | $9^- \to 7^-$ | | 57.38 | 72.72 | 57.38 |
| | $7^- \to 5^-$ | | 59.26 | 73.53 | 58.45 |
| $E3$ | $2_2^+ \to 5^-$ | | — | $1.50\times10^2$ | — |
| | $8^+ \to 5^-$ | | — | 6.08 | — |
| | $3^- \to 0_1^+$ | | — | $3.66\times10^2$ | — |
| | $5^- \to 2_1^+$ | | — | $3.74\times10^1$ | — |
| $E5$ | $5^- \to 0_2^+$ | | $8.53\times10^5$ | $8.69\times10^5$ | $1.35\times10^6$ |
| | $\to 0_1^+$ | | $6.93\times10^5$ | $5.60\times10^5$ | $1.89\times10^5$ |

a) $B(EL)$ values are given in units of $e^2\cdot\text{fm}^{2L}$ and $B(ML)$ values in units of $\mu_0^2\cdot\text{fm}^{2(L-1)}$.
b) These values are calculated with the wave functions for the $\chi^2$-fitting two-body matrix elements 'Level' in Ref. 8).
c) Ref. 43).
d) Ref. 49).
e) Ref. 50).
f) Ref. 20).

measured.[43] As has been mentioned before, this $M1$ transition is forbidden in the $(0g_{9/2}, 1p_{1/2})^4$ configuration space. By including the $1p_{3/2}$ core excitations, non-zero value is given for this transition rate, but the experimental value cannot be explained sufficiently.

The calculated $B(M1)$ for the $4^- \to 5^-$ transition has non-zero value in the calculations A) and B), but vanishes in the $\chi^2$-fitting result. This is caused by the fact that the main component of the lowest $4^-$ state is $|0g^3_{9/2}(v=1, 9/2)\ 1p_{1/2}; 4^-\rangle$ in the calculations A) and B), but $|0g^3_{9/2}(v=3, 7/2)\ 1p_{1/2}; 4^-\rangle$ in the $\chi^2$-fitting result. Since the main component of the $5^-$ state is $|0g^3_{9/2}(v=1, 9/2)\ 1p_{1/2}; 5^-\rangle$ common in all three calculations, the discrepancies of the calculated $B(M1)$ values are caused from the property of the $M1$ operator mentioned before.

In $^{94}$Ru (Table V), the $E2$ transition between the $8^+$ and $6^+$ states is strongly inhibited compared with the same transition in $^{90}$Zr and $^{92}$Mo. Recently, Gloeckner and Serduke[8] have shown that this inhibited transition rate can be explained by the $\chi^2$-fitting calculation which includes the E2 transition rates as a fitting parameter

Table V. Reduced transition probabilities $B(\sigma L)$[a)] in $^{94}$Ru.

| $\sigma L$ | $J_i \to J_f$ | $B(\sigma L)_{\exp}$ | $B(\sigma L)_A$ | $B(\sigma L)_B$ | $B(\sigma L)_{\chi^2}$[b)] |
|---|---|---|---|---|---|
| $M1$ | $4_2^+ \to 4_1^+$ | | 0. | $3.62\times10^{-5}$ | 0. |
| | $4^- \to 5^-$ | | $5.45\times10^{-1}$ | $4.01\times10^{-1}$ | 0. |
| $E2$ | $8^+ \to 6^+$ | $(9.4\pm0.6)\times10^{-2}$ c) | 1.34 | 0.95 | 1.04 |
| | $6^+ \to 4_2^+$ | | 34.47 | 34.24 | 33.81 |
| | $\to 4_1^+$ | $2.56\pm0.24$ c) | 3.98 | 2.85 | 1.99 |
| | $4_2^+ \to 4_1^+$ | | 32.68 | 33.07 | 33.66 |
| | $\to 2^+$ | | 93.53 | 93.28 | 92.98 |
| | $4_1^+ \to 2^+$ | | 6.44 | 4.80 | 2.35 |
| | $2^+ \to 0^+$ | | 77.14 | 79.89 | 78.01 |
| | $11^- \to 9^-$ | | 0. | 111.71 | 79.07 |
| | $9^- \to 7^-$ | | 0. | 126.47 | 95.94 |
| | $7^- \to 5^-$ | | 77.48 | 100.87 | 81.06 |
| | $4^- \to 5^-$ | | 0. | 0.66 | 128.40 |
| $E3$ | $8^+ \to 5^-$ | | — | $1.68\times10^{-1}$ | — |
| | $3^- \to 0^+$ | | — | $5.00\times10^{2}$ | — |
| | $5^- \to 2^+$ | | — | $3.86\times10^{1}$ | — |
| $E5$ | $5^- \to 0^+$ | | $4.89\times10^{5}$ | $2.86\times10^{5}$ | $8.86\times10^{4}$ |

a) $B(EL)$ values are given in units of $e^2\cdot\text{fm}^{2L}$ and $B(ML)$ values in units of $\mu_0^2\cdot\text{fm}^{2(L-1)}$.
b) These values are calculated with the wave functions for the $\chi^2$-fitting two-body matrix elements 'Level' in Ref. 8).
c) Ref. 20).

in the $0g_{9/2}-1p_{1/2}$ configuration space. This inhibition of the $B(E2)$ value is caused by the cancellation between the $E2$ matrix elements of the leading configurations in two states, i.e., $|0g_{9/2}^4(v=2, J)\ 1p_{1/2}^2(0)\ ; J^+\rangle$ and $|0g_{9/2}^6; v=2\ J^+\rangle$, where $J=6$ and 8. In our calculation, the above kind of cancellation is not remarkable in the leading configurations and, although the introduction of the core excitations improves this situation, the reduction of the $E2$ matrix element is not accomplished sufficiently.

The drastic discrepancies exist among the $B(E2)$ values for the transitions between some negative parity levels obtained respectively by the calculations A), B) and $\chi^2$-fitting. These are caused by the differences of the composition in the wave functions of the $4^-$ and $9^-$ states among three calculations and by the properties of the matrix element of single particle even tensor operator in the seniority scheme at the middle of the shell, i.e., $(0g_{9/2}^5;\ vJ'\|E2\|0g_{9/2}^5;\ vJ)=0$ and $(0g_{9/2}^5;\ vJ'\|E2\|0g_{9/2}^5;\ v-2\ J)\neq0$. The main component of the lowest $4^-$ state is $|0g_{9/2}^5(v=1, 9/2)\ 1p_{1/2}; 4^-\rangle$ in the calculations A) and B), but $|0g_{9/2}^5(v=3, 7/2)\ 1p_{1/2}; 4^-\rangle$ in the $\chi^2$-fitting result. Since the main component in the $5^-$ state is $|0g_{9/2}^5(v=1, 9/2)\ 1p_{1/2}; 5^-\rangle$ common in all three calculations, the calculated $B(E2)$ for the $4^-\to5^-$ transition is very small in the calculations A) and B) but large in the $\chi^2$-fitting calculation as a result of the above properties of the $E2$ matrix element. The main component of the lowest $9^-$ state is $|0g_{9/2}^5(v=3, 17/2)\ 1p_{1/2}; 9^-\rangle$

Table VI. Reduced transition probabilities $B(\sigma L)$[a] in $^{89}$Y.

| $\sigma L$ | $J_i \to J_f$ | $B(\sigma L)_{\text{exp.}}$ | $B(\sigma L)_A$ | $B(\sigma L)_B$ | $B(\sigma L)_{\chi^2}$ |
|---|---|---|---|---|---|
| $M1$ | $3/2_2^- \to 1/2^-$ | | — | 0.24 | — |
| | $5/2^- \to 3/2_1^-$ | | — | 0.04 | — |
| | $3/2_1^- \to 1/2^-$ | | — | 1.36 | — |
| | $9/2_2^+ \to 9/2_1^+$ | | — | 0.02 | — |
| | $11/2^+ \to 9/2_1^+$ | | — | 0.13 | — |
| | $7/2_1^+ \to 5/2^+$ | | — | $3.41\times10^{-3}$ | — |
| | $\to 9/2_1^+$ | | — | 0.06 | — |
| $E2$ | $3/2_1^- \to 1/2^-$ | 65.59[b] | — | 19.16 | — |
| | $13/2^+ \to 9/2_2^+$ | | — | 2.84 | — |
| | $\to 9/2_1^+$ | | — | 32.66 | — |
| | $9/2_2^+ \to 9/2_1^+$ | | — | 17.22 | — |
| | $5/2^+ \to 9/2_1^+$ | | — | 31.58 | — |
| $E3$ | $5/2^- \to 9/2_1^+$ | | — | 589.73 | — |
| | $3/2_1^- \to 9/2_1^+$ | | — | 38.80 | — |
| | $7/2_2^+ \to 1/2^-$ | $5.15\times10^4$ [b],[c] | — | $6.60\times10^2$ | — |
| | $7/2_1^+ \to 1/2^-$ | $3.66\times10^4$ [b],[c] | — | $1.29\times10^3$ | — |
| | $5/2^+ \to 1/2^-$ | $2.58\times10^4$ [b],[c] | — | $1.97\times10^3$ | — |
| $M4$ | $9/2_1^+ \to 1/2^-$ | $5.32\times10^4$ [b] | $5.09\times10^5$ [d] | $5.72\times10^5$ | $5.09\times10^5$ [d] |

a) $B(EL)$ values are given in units of $e^2\cdot\text{fm}^{2L}$ and $B(ML)$ values in units of $\mu_0^2\cdot\text{fm}^{2(L-1)}$.
b) Ref. 26).
c) Ref. 51).
d) Single particle value $|(0g_{9/2}\|M4\|1p_{1/2})|^2/10$.

in the calculation A), but $|0g_{9/2}^5(v=5, 17/2)\ 1p_{1/2}; 9^-\rangle$ in the calculations B) and $\chi^2$-fitting. Since the main component in the $11^-$ and $7^-$ states has the form $|0g_{9/2}^5(v=3, J')\ 1p_{1/2}; J^-\rangle$, where $J'=21/2$ for $J=11$ and $J'=13/2$ for $J=7$, the differences of the $B(E2)$ values for the $11^-\to9^-$ and $9^-\to7^-$ transitions among three cases reduce also to the properties of the $E2$ matrix element mentioned above.

## 4.2. *Transition rates in odd Z nuclei*

In $^{89}$Y (Table VI), the $B(E2)$ value is measured for the transition from the first $3/2^-$ state, which is regarded as $2p$-$1h$ state,[28),29)] to the ground state. For this transition, the $B(E2)$ value calculated from the matrix element between the respective main components $|1p_{1/2}; 1/2^-\rangle$ and $|1p_{1/2}^2(0)\ 1p_{3/2}^{-1}; 3/2^-\rangle$, is 35.85 $e^2\cdot\text{fm}^4$. The mixing of the $|0g_{9/2}^2(0)\ 1p_{3/2}^{-1}; 3/2^-\rangle$ configuration in the first $3/2^-$ state reduces the calculated $B(E2)$ from the above value.

All of three measured $E3$ transitions in this nucleus are very strong. It can also be seen from Table VI that the calculated $B(E3)$ corresponding to the measured ones are large compared with those for other possible transitions. Especially, in this sense, the large $B(E3)$ values for the $5/2^+\to1/2^-$ and $7/2_1^+\to1/2^-$ transitions are qualitatively explained with our model. In the weak-coupling model,[25)] the first $5/2^+$ and the first $7/2^+$ states are interpreted as the members of states constructed from the coupling of the first $2^+$ state in the $^{88}$Sr core and one proton in the $0g_{9/2}$ orbit, i.e., $|2^+ \otimes 0g_{9/2}; J^+\rangle$. Since the ground $1/2^-$ state is the state constructed from the coupling of the $^{88}$Sr ground state and the $1p_{1/2}$ proton, i.e., $|0^+ \otimes 1p_{1/2}; 1/2^-\rangle$, the $E3$ transition from two states considered above to the ground state is forbidden in this model.

The $B(M4)$ value between the first $9/2^+$ and the ground $1/2^-$ states in this nucleus is also calculated and compared with the experimental one.[26] The inclusion of the $1p_{3/2}$ core excitations gives the slight enlargement of $B(M4)$ value from the single-particle value [$B(M4)_A$ in column 5].

The inclusion of the $1p_{3/2}$ core excitations gives a remarkable effect on the $B(M1)$ values in $^{91}$Nb as well (Table VII). Concerning the transitions between the negative parity states, it is seen from the comparison of the $B(M1)_A$ and $B(M1)_B$ that the effect of the $1p_{3/2}$ core excitations is not uniform in each transition, i.e., some transitions are enhanced and the others are hindered. Especially, the

Table VII. Reduced transition probabilities $B(\sigma L)^{a)}$ in $^{91}$Nb.

| $\sigma L$ | $J_i \to J_f$ | $B(\sigma L)_{\rm exp}$ | $B(\sigma L)_A$ | $B(\sigma L)_B$ | $B(\sigma L)_{\chi^2}$ b) |
|---|---|---|---|---|---|
| $M1$ | $11/2^+ \to 13/2^+$ | | 0. | $6.63\times10^{-3}$ | 0. |
| | $9/2_2^+ \to 9/2_1^+$ | | 0. | $4.31\times10^{-5}$ | 0. |
| | $\to 7/2^+$ | | 0. | $3.08\times10^{-3}$ | 0. |
| | $7/2^+ \to 9/2_1^+$ | | 0. | $5.24\times10^{-4}$ | 0. |
| | $15/2^- \to 17/2^-$ | | $5.25\times10^{-1}$ | 1.26 | $5.25\times10^{-1}$ |
| | $11/2^- \to 13/2^-$ | | $5.34\times10^{-1}$ | $5.22\times10^{-1}$ | $5.34\times10^{-1}$ |
| | $\to 9/2^-$ | | 0. | $4.22\times10^{-1}$ | 0. |
| | $3/2^- \to 5/2^-$ | | $5.95\times10^{-1}$ | $7.61\times10^{-2}$ | $5.95\times10^{-1}$ |
| | $\to 1/2^-$ | | 0. | 1.04 | 0. |
| $E2$ | $21/2^+ \to 17/2^+$ | $106\pm11$ c) | 33.05 | 50.72 | 33.05 |
| | $17/2^+ \to 13/2^+$ | | 57.38 | 105.64 | 57.38 |
| | $13/2^+ \to 9/2_2^+$ | | 57.25 | 101.77 | 40.93 |
| | $\to 9/2_1^+$ | | 2.02 | 10.52 | 17.40 |
| | $9/2_2^+ \to 7/2^+$ | | 78.09 | 150.20 | 59.45 |
| | $17/2^- \to 13/2^-$ | $32.0\pm1.9$ d) | 16.53 | 21.38 | 16.53 |
| | $13/2^- \to 9/2^-$ | $71.1\pm3.2$ e) | 41.27 | 55.31 | 41.27 |
| | $9/2^- \to 5/2^-$ | $\leq 178$ f) | 59.68 | 77.12 | 59.68 |
| | $5/2^- \to 1/2^-$ | | 51.94 | 66.38 | 51.94 |
| $M4$ | $1/2^- \to 9/2_1^+$ | $2.60\times10^5$ f) | $1.92\times10^5$ | $2.34\times10^5$ | $3.18\times10^4$ |

a) $B(EL)$ values are given in units of $e^2\cdot{\rm fm}^{2L}$ and $B(ML)$ values in units of $\mu_0^2\cdot{\rm fm}^{2(L-1)}$.
b) These values are calculated with the wave functions for the $\chi^2$-fitting two-body matrix elements 'Level' in Ref. 8).
c) Ref. 41).
d) Ref. 40).
e) Ref. 52).
f) Ref. 31).

$B(M1)$ for the $3/2^- \to 1/2^-$ transition calculated with the $1p_{3/2}$ core excitations [calculation B)] has relatively large value, whereas the value in the $0g_{9/2}-1p_{1/2}$ configuration space vanishes [calculations A) and $\chi^2$-fitting].

The stretched $E2$ cascade $21/2^+ \to 17/2^+ \to 13/2^+ \to 9/2_1^+$ is observed in $^{91}$Nb.[30),40)] The $E2$ transitions between these positive parity states are considerably enhanced by the $1p_{3/2}$ core excitations (Table VII). In the $(0g_{9/2}, 1p_{1/2})^3$ configuration space, the strengths of the transitions in the $E2$ cascade $17/2^- \to 13/2^- \to 9/2^- \to 5/2^- \to 1/2^-$ in $^{91}$Nb are theoretically almost equivalent to the corresponding strengths of the transitions in the $E2$ cascade $8^+ \to 6^+ \to 4^+ \to 2^+ \to 0^+$ in $^{90}$Zr or $^{92}$Mo. Note that the experimental $B(E2)$ values for the $17/2^- \to 13/2^-$ and $13/2^- \to 9/2^-$ transitions in $^{91}$Nb have very similar values to the experimental ones for the $8^+ \to 6^+$ and $6^+ \to 4^+$ transitions in $^{92}$Mo (Table III).

We calculate also the $M4$ transition rate between the isomeric first $1/2^-$ and the ground $9/2^+$ states in $^{91}$Nb. The agreement with the experimental value is good in the calculation B).

In $^{93}$Tc (Table VIII), the $B(M1)$ value for the $3/2^- \to 1/2^-$ transition is enhanced largely with the $1p_{3/2}$ core excitations as like as the same transition in $^{91}$Nb. In the high-spin negative parity states, the effect of the core excitations is

Table VIII. Reduced transition probabilities $B(\sigma L)$[a)] in $^{93}$Tc.

| $\sigma L$ | $J_i \to J_f$ | $B(\sigma L)_{\rm exp}$ | $B(\sigma L)_A$ | $B(\sigma L)_B$ | $B(\sigma L)_{\chi^2}$[b)] |
|---|---|---|---|---|---|
| $M1$ | $9/2_2^+ \to 9/2_1^+$ | | 0. | $2.53\times10^{-8}$ | 0. |
| | $11/2^+ \to 13/2^+$ | | 0. | $7.19\times10^{-7}$ | 0. |
| | $\to 9/2_1^+$ | | 0. | $3.17\times10^{-6}$ | 0. |
| | $7/2^+ \to 9/2_1^+$ | | 0. | $2.09\times10^{-5}$ | 0. |
| | $3/2^- \to 5/2^-$ | | $5.95\times10^{-1}$ | $9.03\times10^{-2}$ | $5.95\times10^{-1}$ |
| | $\to 1/2^-$ | | 0. | 1.16 | 0. |
| $E2$ | $21/2^+ \to 17/2^+$ | $65.9\pm4.0$[c)] | 32.35 | 30.09 | 23.89 |
| | $17/2^+ \to 13/2^+$ | | 56.17 | 51.65 | 41.12 |
| | $13/2^+ \to 9/2_1^+$ | | 59.26 | 62.33 | 61.89 |
| | $7/2^+ \to 9/2_1^+$ | | 101.23 | 106.31 | 108.50 |
| | $25/2^- \to 21/2^-$ | | 44.91 | 57.55 | 44.91 |
| | $21/2^- \to 17/2^-$ | | 59.40 | 76.83 | 62.15 |
| | $17/2^- \to 13/2^-$ | $11.4\pm0.9$[d)] | 1.42 | 12.49 | 2.81 |
| | $13/2^- \to 9/2^-$ | | 4.25 | 80.10 | 34.82 |
| | $9/2^- \to 5/2^-$ | | 6.89 | 126.71 | 96.14 |
| | $5/2^- \to 1/2^-$ | | 77.40 | 96.83 | 78.79 |
| $M4$ | $1/2^- \to 9/2_1^+$ | $4.21\times10^{5}$[e)] | $6.10\times10^{5}$ | $6.83\times10^{5}$ | $5.75\times10^{4}$ |

a) $B(EL)$ values are given in units of $e^2\cdot{\rm fm}^{2L}$ and $B(ML)$ values in units of $\mu_0^2\cdot{\rm fm}^{2(L-1)}$.
b) These values are calculated with the wave functions for the $\chi^2$-fitting two-body matrix elements 'Level' in Ref. 8).
c) Ref. 41).
d) Ref. 39).
e) Ref. 34).

more complicated than the case of $^{91}$Nb. These complicated features are reflected clearly on the calculated results of the $B(E2)$ value rather than the $B(M1)$ value.

From the comparison of the theoretical $B(E2)$ values of the negative parity states in the calculations A) and B), it is seen that the values for the $17/2^- \to 13/2^-$, $13/2^- \to 9/2^-$ and $9/2^- \to 5/2^-$ transitions are much enhanced by the $1p_{3/2}$ core excitations. Especially, the $17/2^- \to 13/2^-$ transition rate is well explained. In the $17/2^-$ and $13/2^-$ states, various core excited states which have the seniority four for the $(0g_{9/2})^4$ term, i.e., $|0g^4_{9/2}(v=4, J')1p^2_{1/2}(0)\ 1p^{-1}_{3/2};\ J^-\rangle$, are mixed sizably and the $E2$ matrix elements between these configurations give the constructive effect on the $B(E2)$ value altogether. On the other hand, the enhancements of the $13/2^- \to 9/2^-$ and $9/2^- \to 5/2^-$ transitions are given by the slight different mechanism from the above case. By including the $1p_{3/2}$ core excitations, the $9/2^-$ state which has the configuration $|0g^4_{9/2}(v=4, 4)\ 1p_{1/2}; 9/2^-\rangle$ as a main component is lowered strongly rather than the state which has the configuration $|0g^4_{9/2}(v=2, 4)\,1p_{1/2};\ 9/2^-\rangle$ as a main component and, then, the former becomes the lowest $9/2^-$ state reversing the order of two states in the calculation A). Since the core excited configurations which have the seniority four are mixed sizably in the $5/2^-$, $9/2^-$ and $13/2^-$ states, the large enhancement occurs in the $E2$ transitions between these states.

The $B(M4)$ value is also well explained by our calculation in this nucleus.

## § 5. Conclusion

We have calculated the energy levels and various transition rates of the $N=50$ nuclei with the configuration space including one and two proton core excitations from the $1p_{3/2}$ orbit in addition to the $(0g_{9/2}, 1p_{1/2})^n$ configuration.

On the explanation of the low-lying energy level structures, the $(0g_{9/2}, 1p_{1/2})^n$ configuration is good approximation as denoted by many authors.[3)~8)] The $1p_{3/2}$ core excitations, however, produce the remarkable effects on some specific energy levels. The second $2^+$ state in $^{90}$Zr, the second $3/2^-$ and the first $7/2^+$ states in $^{91}$Nb and almost all the low-lying levels in $^{89}$Y, etc., are well explained with the $1p_{3/2}$ core excitations. It is also seen that the effect of the $1p_{3/2}$ core excitations on the energy levels is diminished with the growth of proton number.

An important effect of including the $1p_{3/2}$ core excitations appears more clearly on the transition rates. The $E3$ and some $M1$ transitions, which are forbidden in the $0g_{9/2}-1p_{1/2}$ configuration space, can be explained to some extent by including the $1p_{3/2}$ core excitations. In the other transitions, the inclusion of the $1p_{3/2}$ core excitations improves the calculated transition rates compared with the results in the $0g_{9/2}-1p_{1/2}$ configuration space.

Furthermore, in some levels in the heavier nuclei (e.g., the first $7/2^-$ and the first $9/2^-$ states in $^{93}$Tc and the first $9^-$ state in $^{94}$Ru, etc.), the high seniority state becomes dominant in the wave function of these states by the influence of the core excitations. Consequently, the calculated transition rates associated with the above states are enhanced largely compared with the ones without the core excitations. This change of the roles of the low and high seniority states in the levels mentioned above is consistent with the result of the $\chi^2$-fitting method in the $0g_{9/2}-1p_{1/2}$ configuration space.[8)]

In our calculations, the single-particle energy difference between the $1p_{1/2}$ and $1p_{3/2}$ orbits was taken to be 0.60 MeV. This value is smaller (about one-half) than the usual one.[11),53),54)] Since, as mentioned in § 3, the attractive part of the two-body matrix elements of the K-K interaction is rather large, it was necessary to take the small value for the single-particle energy difference $\varepsilon(1p_{1/2})-\varepsilon(1p_{3/2})$ in order that the $1p_{3/2}$ core excitations may be effective.

The authors wish to thank Professor T. Sebe of Hosei University for reading the manuscript and making several suggestions. They gratefully acknowledge many useful discussions with Dr. K. Arita.

## References


1) K. W. Ford, Phys. Rev. **98** (1955), 1516.
2) B. F. Bayman, A. S. Reiner and R. K. Sheline, Phys. Rev. **115** (1959), 1627.
3) I. Talmi and I. Unna, Nucl. Phys. **19** (1960), 225.
4) N. Auerbach and I. Talmi, Nucl. Phys. **64** (1965), 458.
5) J. Vervier, Nucl. Phys. **75** (1966), 17.
6) D. H. Gloeckner, M. H. Macfarlane, R. D. Lawson and F. J. D. Serduke, Phys. Letters **40B** (1972), 597.
7) J. B. Ball, J. B. McGrory and J. S. Larsen, Phys. Letters **41B** (1972), 581.
8) D. H. Gloeckner and F. J. D. Serduke, Nucl. Phys. **A220** (1974), 477.
9) K. Fujita and T. Komoda, Prog. Theor. Phys. **57** (1977), 692.
10) C. Dedes and J. M. Irvine, J. Phys. G: Nucl. Phys. **1** (1975), 865.
11) C. Dedes, J. Phys. G: Nucl. Phys. **2** (1976), L25.
12) W. J. Courtney and H. T. Fortune, Phys. Letters **41B** (1972), 4.
13) J. D. Vergados and T. T. S. Kuo, Nucl. Phys. **A168** (1971), 225.
14) A. Kallio and K. Kolltveit, Nucl. Phys. **53** (1964), 87.
15) T. Engeland and A. Kallio, Nucl. Phys. **59** (1964), 211.
16) S. A. Moszkowski and B. L. Scott, Ann. of Phys. **11** (1960), 65.
17) B. C. Carlson and I. Talmi, Phys. Rev. **96** (1954), 436.
18) D. C. Kocher, Nuclear Data Sheets **16** (1975), 55.
19) D. C. Kocher and D. J. Horen, Nuclear Data Sheets **B7** (1972), 299.
20) C. M. Lederer, J. M. Jaklevic and J. M. Hollander, Nucl. Phys. **A169** (1971), 449.
21) A. Arima and H. Horie, Prog. Theor. Phys. **12** (1954), 623.
22) H. Noya, A. Arima and H. Horie, Prog. Theor. Phys. Suppl. No. 8 (1958), 33.
23) C. Dedes and J. M. Irvine, J. Phys. G: Nucl. Phys. **1** (1975), 929.
24) D. C. Kocher, Nuclear Data Sheets **10** (1973), 241.
25) P. Hoffman-Pinther and J. L. Adams, Nucl. Phys. **A229** (1974), 365.
26) D. C. Kocher, Nuclear Data Sheets **16** (1975), 445.
27) L. Hulstman, H. P. Blok, J. Verburg, J. G. Hoogteyling, C. B. Nederveen, H. T. Vijlbrief, E. J. Kaptein, S. W. L. Milo and J. Blok, Nucl. Phys. **A251** (1975), 269.
28) C. D. Kavaloski, J. S. Lilley, D. C. Shreve and N. Stein, Phys. Rev. **161** (1967), 1107.
29) B. M. Preedom, E. Newman and J. C. Hiebert, Phys. Rev. **166** (1968), 1156.

30) M. Grecescu, A. Nilsson and L. Harms-Ringdahl, Nucl. Phys. **A212** (1973), 429.
31) H. Verheul and W. B. Ewbank, Nuclear Data Sheets **B8** (1972), 477.
32) J. L. Horton, C. L. Hollas, P. J. Riley, S. A. A. Zaidi, C. M. Jones and J. L. C. Ford, Jr., Nucl. Phys. **A190** (1972), 362.
33) R. Chapman, J. E. Kitching and W. Mclatchie, Nucl. Phys. **A196** (1972), 347.
34) D. C. Kocher, Nuclear Data Sheets **B8** (1972), 527.
35) R. L. Kozub and D. H. Youngblood, Phys. Rev. **C4** (1971), 535.
36) Y. Shamai, D. Ashery, A. I. Yavin, G. Bruge and A. Chaumeaux, Nucl. Phys. **A197** (1972), 211.
37) J. Bommer, H. Fuchs, K. Grabish, H. Kluge and G. Roschert, Nucl. Phys. **A173** (1971), 383.
38) P. J. Riley, J. L. Horton, C. L. Hollas, S. A. A. Zaidi, C. M. Jones and J. L. C. Ford, Jr., Phys. Rev. **C4** (1971), 1864.
39) B. A. Brown, D. B. Fossan, P. M. S. Lesser and A. R. Poletti, Phys. Rev. **C13** (1976), 1194.
40) B. A. Brown, P. M. S. Lesser and D. B. Fossan, Phys. Rev. **C13** (1976), 1900.
41) W. D. Schneider, K. H. Gonsior and C. Günther, Nucl. Phys. **A249** (1975), 103.
42) J. Bellicard, P. Leconte, T. H. Curtis, R. A. Eisenstein, D. Madsen and C. Bockelman, Nucl. Phys. **A143** (1970), 213.
43) C. T. Papadopoulos, A. G. Hartas, P. A. Assimakopoulos, G. Andritsopoulos and N. H. Gaugas, Nucl. Phys. **A254** (1975), 93.
44) A. B. Tucker and S. O. Simmons, Nucl. Phys. **A156** (1970), 83.
45) R. P. Singhal, S. W. Brain, W. A. Gillespie, A. Johnston, E. W. Lees and A. G. Slight, Nucl. Phys. **A218** (1974), 189.
46) K. G. Löbner, Nucl. Phys. **58** (1964), 49.
47) Phan-Xuan-Ho, J. Bellicard, P. Leconte and I. Sick, Nucl. Phys. **A210** (1973), 189.
48) R. Bauer, P. Ring and J. Speth, *Contributions to International Conference on Nuclear Physics, Munich, 1973,* p. 106.
49) S. Cochavi, J. M. McDonald and D. B. Fossan, Phys. Rev. **C3** (1971), 1352.
50) P. H. Stelson and L. Grodzins, Nuclear Data **A1** (1965), 21.
51) S. P. Fivozinsky, S. Penner, J. W. Lightbody, Jr. and D. Blum, Phys. Rev. **C9** (1974), 1533.
52) C. V. K. Baba, D. B. Fossan, T. Faestermann, F. Feilitzsch, M. R. Maier, P. Raghavan, R. S. Raghavan and C. Signorini, Nucl. Phys. **A257** (1976), 135.
53) B. Sorensen, Nucl. Phys. **A177** (1971), 465.
54) R. J. Lombard, Nucl. Phys. **A117** (1968), 365.